2014-12-09

A calcium-dependent protease as a potential therapeutic target for Wolfram syndrome

Simin Lu
University of Massachusetts Medical School

Et al.

A calcium-dependent protease as a potential therapeutic target for Wolfram syndrome

Simin Lu[a,b], Kohsuke Kanekura[a], Takashi Hara[a], Jana Mahadevan[a], Larry D. Spears[a], Christine M. Oslowski[c], Rita Martinez[d], Mayu Yamazaki-Inoue[e], Masashi Toyoda[e], Amber Neilson[d], Patrick Blanner[d], Cris M. Brown[a], Clay F. Semenkovich[a], Bess A. Marshall[f], Tamara Hershey[g], Akihiro Umezawa[e], Peter A. Greer[h], and Fumihiko Urano[a,i,1]

[a]Department of Medicine, Division of Endocrinology, Metabolism, and Lipid Research, Washington University School of Medicine, St. Louis, MO 63110; [b]Graduate School of Biomedical Sciences, University of Massachusetts Medical School, Worcester, MA 01655; [c]Department of Medicine, Boston University School of Medicine, Boston, MA 02118; [d]Department of Genetics, iPSC core facility, Washington University School of Medicine, St. Louis, MO 63110; [e]Department of Reproductive Biology, National Center for Child Health and Development, Tokyo 157-8535, Japan; [f]Department of Pediatrics, Washington University School of Medicine, St. Louis, MO 63110; [g]Departments of Psychiatry, Neurology, and Radiology, Washington University School of Medicine, St. Louis, MO 63110; [h]Department of Pathology and Molecular Medicine, Queen's University, Division of Cancer Biology and Genetics, Queen's Cancer Research Institute, Kingston, Ontario K7L3N6, Canada; and [i]Department of Pathology and Immunology, Washington University School of Medicine, St. Louis, MO 63110

Edited by Stephen O'Rahilly, University of Cambridge, Cambridge, United Kingdom, and approved November 7, 2014 (received for review November 4, 2014)

Wolfram syndrome is a genetic disorder characterized by diabetes and neurodegeneration and considered as an endoplasmic reticulum (ER) disease. Despite the underlying importance of ER dysfunction in Wolfram syndrome and the identification of two causative genes, Wolfram syndrome 1 (*WFS1*) and Wolfram syndrome 2 (*WFS2*), a molecular mechanism linking the ER to death of neurons and β cells has not been elucidated. Here we implicate calpain 2 in the mechanism of cell death in Wolfram syndrome. Calpain 2 is negatively regulated by WFS2, and elevated activation of calpain 2 by WFS2-knockdown correlates with cell death. Calpain activation is also induced by high cytosolic calcium mediated by the loss of function of WFS1. Calpain hyperactivation is observed in the WFS1 knockout mouse as well as in neural progenitor cells derived from induced pluripotent stem (iPS) cells of Wolfram syndrome patients. A small-scale small-molecule screen targeting ER calcium homeostasis reveals that dantrolene can prevent cell death in neural progenitor cells derived from Wolfram syndrome iPS cells. Our results demonstrate that calpain and the pathway leading its activation provides potential therapeutic targets for Wolfram syndrome and other ER diseases.

Wolfram syndrome | endoplasmic reticulum | diabetes | neurodegeneration | treatment

The endoplasmic reticulum (ER) takes center stage for protein production, redox regulation, calcium homeostasis, and cell death (1, 2). It follows that genetic or acquired ER dysfunction can trigger a variety of common diseases, including neurodegenerative diseases, metabolic disorders, and inflammatory bowel disease (3, 4). Breakdown in ER function is also associated with genetic disorders such as Wolfram syndrome (5–8). It is challenging to determine the exact effects of ER dysfunction on the fate of affected cells in common diseases with polygenic and multifactorial etiologies. In contrast, we reasoned that it should be possible to define the role of ER dysfunction in mechanistically homogenous patient populations, especially in rare diseases with a monogenic basis, such as Wolfram syndrome (9).

Wolfram syndrome (OMIM 222300) is a rare autosomal recessive disorder characterized by juvenile-onset diabetes mellitus and bilateral optic atrophy (7). Insulin-dependent diabetes usually occurs as the initial manifestation during the first decade of life, whereas the diagnosis of Wolfram syndrome is invariably later, with onset of symptoms in the second and ensuing decades (7, 10, 11). Two causative genes for this genetic disorder have been identified and named Wolfram syndrome 1 (*WFS1*) and Wolfram syndrome 2 (*WFS2*) (12, 13). It has been shown that multiple mutations in the *WFS1* gene, as well as a specific mutation in the *WFS2* gene, lead to β cell death and neurodegeneration through ER and mitochondrial dysfunction (5, 6, 14–16). *WFS1* gene variants are also associated with a risk of type 2 diabetes (17). Moreover, a specific *WFS1* variant can cause autosomal dominant diabetes (18), raising the possibility that this rare disorder is relevant to common molecular mechanisms altered in diabetes and other human chronic diseases in which ER dysfunction is involved.

Despite the underlying importance of ER malfunction in Wolfram syndrome, and the identification of *WFS1* and *WFS2* genes, a molecular mechanism linking the ER to death of neurons and β cells has not been elucidated. Here we show that the calpain protease provides a mechanistic link between the ER and death of neurons and β cells in Wolfram syndrome.

Results

The causative genes for Wolfram syndrome, *WFS1* and *WFS2*, encode transmembrane proteins localized to the ER (5, 12, 13). Mutations in the *WFS1* or *WFS2* have been shown to induce neuronal and β cell death. To determine the cell death pathways emanating from the ER, we sought proteins associated with Wolfram syndrome causative gene products. HEK293 cells were transfected with a GST-tagged WFS2 expression plasmid. The GST-WFS2 protein was purified along with associated proteins on a glutathione affinity resin. These proteins were separated by

Significance

Wolfram syndrome is an autosomal recessive disorder characterized by juvenile diabetes and neurodegeneration, and is considered a prototype of human endoplasmic reticulum (ER) disease. Wolfram syndrome is caused by loss of function mutations of Wolfram syndrome 1 or Wolfram syndrome 2 genes, which encode transmembrane proteins localized to the ER. Despite its rarity, Wolfram syndrome represents the best human disease model currently available to identify drugs and biomarkers associated with ER health. Furthermore, this syndrome is ideal for studying the mechanisms of ER stress-mediated death of neurons and β cells. Here we report that the pathway leading to calpain activation offers potential drug targets for Wolfram syndrome and substrates for calpain might serve as biomarkers for this syndrome.

Author contributions: S.L., P.A.G., and F.U. designed research; S.L., K.K., T. Hara, J.M., L.D.S., C.M.O., R.M., M.Y.-I., M.T., A.N., P.B., and C.M.B. performed research; S.L., B.A.M., T. Hershey, A.U., and F.U. contributed new reagents/analytic tools; S.L., K.K., T. Hara, J.M., L.D.S., C.M.O., R.M., M.Y.-I., M.T., A.N., P.B., C.M.B., C.F.S., P.A.G., and F.U. analyzed data; and S.L., C.F.S., P.A.G., and F.U. wrote the paper.

The authors declare no conflict of interest.

This article is a PNAS Direct Submission.

Freely available online through the PNAS open access option.

[1]To whom correspondence should be addressed. Email: urano@dom.wustl.edu.

This article contains supporting information online at www.pnas.org/lookup/suppl/doi:10.1073/pnas.1421055111/-/DCSupplemental.

SDS/PAGE and visualized by Coomassie staining. Matrix-assisted laser desorption/ionization-time of flight (MALDI-TOF) mass spectroscopic analysis revealed 13 interacting proteins (Table S1), and one of the WFS2-associated polypeptides was CAPN2, the catalytic subunit of calpain 2, a member of the calcium dependent cysteine proteases family whose members mediate diverse biological functions including cell death (19–21) (Fig. 1*A*). Previous studies have shown that calpain 2 activation is regulated on the ER membrane and it plays a role in ER stress-induced apoptosis and β cell death (20, 22–24), which prompted us to study the role of WFS2 in calpain 2 activation.

Calpain 2 is a heterodimer consisting the CAPN2 catalytic subunit and the CAPNS1 (previously known as CAPN4) regulatory subunit. We first verified that WFS2 interacts with calpain 2 by showing that endogenous calpain 2 subunits CAPN2 (Fig. 1*B*) and CAPNS1 (Fig. 1*C*) each associated with GST-tagged WFS2 expressed in HEK293 cells. Endogenous CAPN2 was also found to be coimmunoprecipated with N- or C-terminal FLAG-tagged WFS2 expressed in HEK293 cells (Fig. S1 *A* and *B*, respectively). To further confirm these findings, we performed a coimmunoprecipitation experiment in Neuro2a cells (a mouse neuroblastoma cell line) and INS-1 832/13 cells (a rat pancreatic β cell line)

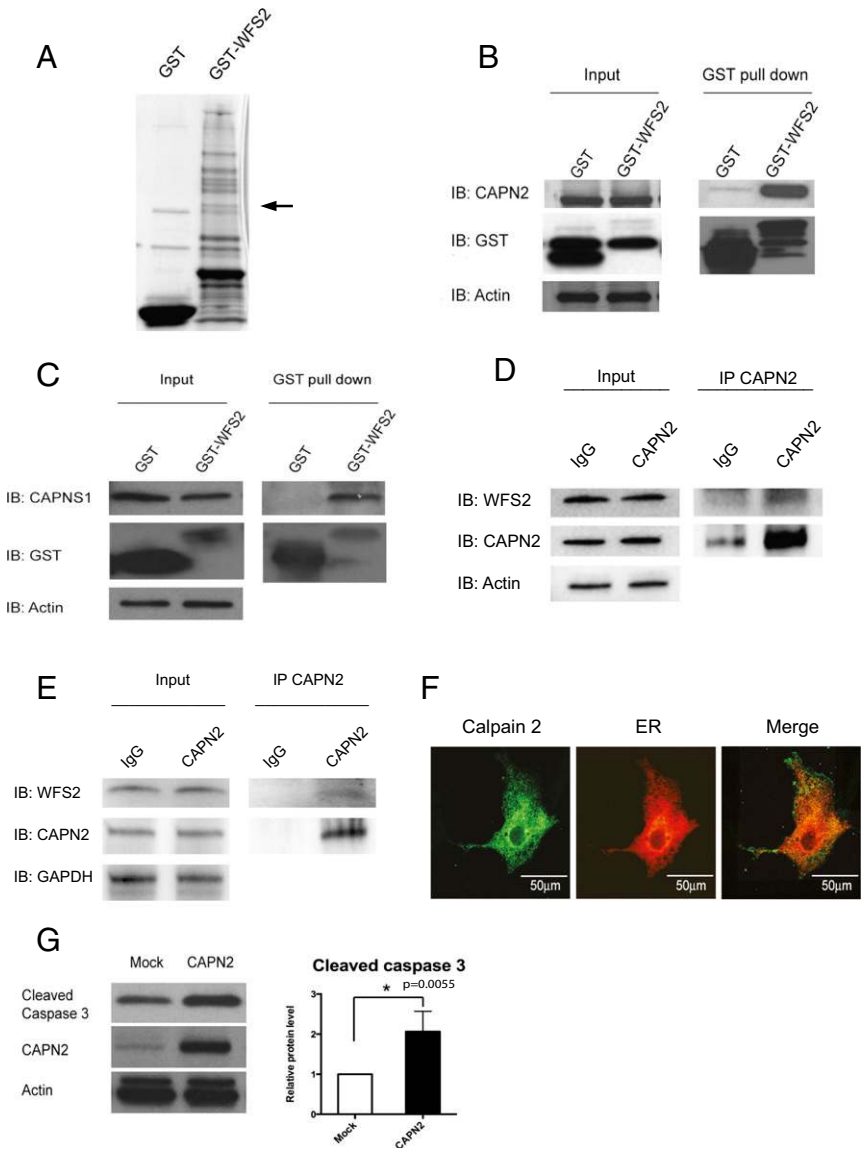

Fig. 1. WFS2 interacts with CAPN2. (*A*) Affinity purification of WFS2-associated proteins from HEK293 cells transfected with GST or GST-WFS2 expression plasmid. Proteins were separated by SDS/PAGE and visualized by Coomassie blue staining. CAPN2 was identified by MALDI-TOF analysis and denoted by an arrow. (*B*) GST-tagged WFS2 was pulled down on a glutathione affinity resin from lysates of HEK293 cells transfected with a GST-WFS2 expression plasmid, and the pulled-down products were analyzed for CAPN2 by immunoblotting with anti-CAPN2 antibody. (*C*) GST-tagged WFS2 was pulled down on a glutathione affinity resin from lysates of HEK293 cells transfected with GST-WFS2 expression plasmid and the pulled-down products were analyzed for CAPNS1 by immunoblotting with anti-CAPNS1 antibody. (*D*) Lysates of Neuro2a cells were immunoprecipitated with IgG or anti-calpain 2 antibodies. Lysates of IgG and anti-calpain 2 immunoprecipitates were analyzed for WFS2, CAPN2 or actin by immunoblotting. (*E*) Lysates of INS-1 832/13 cells were immunoprecipitated with IgG or anti-calpain 2 antibody. Lysates of IgG and anti-calpain 2 immunoprecipitates were analyzed for WFS2, CAPN2 or actin by immunoblotting. (*F*) COS7 cells were transfected with pDsRed2-ER vector (*Center*) and stained with anti-calpain 2 antibody (*Left*). (*Right*) A merged image is shown. (*G*) HEK293 cells were transfected with empty expression plasmid or a CAPN2 expression plasmid. Apoptosis was monitored by immunoblotting analysis of caspase 3 cleavage. (*Left*) Expression levels of CAPN2 and actin were measured by immunoblotting. (*Right*) Quantification of immunoblot is shown ($n = 3$, $^*P < 0.05$).

and found that endogenous WFS2 interacted with endogenous CAPN2 (Fig. 1 *D* and *E*). WFS2 is known to be a transmembrane protein localized to the ER. We therefore explored the possibility that calpain 2 might also localize to the ER. We transfected COS7 cells with pDsRed2-ER vector to visualize ER. Immunofluorescence staining of COS7 cells showed that endogenous calpain 2 was mainly localized to the cytosol, but also showed that a small portion colocalized with DsRed2-ER protein at the ER (Fig. 1*F*). Cell fractionation followed by immunoblot further confirmed this observation (Fig. S1*C*). Collectively, these results suggest that calpain 2 interacts with WFS2 at the cytosolic face of the ER.

Calpain hyperactivation has been shown to contribute to cell loss in various diseases (19), raising the possibility that calpain 2 might be involved in the regulation of cell death. To verify this issue, we overexpressed CAPN2, the catalytic subunit of calpain 2, and observed increase of cleaved caspase-3 in HEK293 cells indicating that hyperactivation of calpain 2 induces cell death (Fig. 1*G*).

To determine whether WFS2 plays a role in cell survival, we suppressed WFS2 expression in mouse neuronal NSC34 cells using siRNA and measured cell death under normal and ER stress conditions. WFS2 knockdown was associated with increased cleavage of caspase-3 in normal or ER stressed conditions (Fig. 2 *A* and *B*). We subsequently evaluated calpain 2 activation by measuring the cleavage of alpha II spectrin, a substrate for calpain 2. RNAi-mediated knockdown of WFS2 induced calpain activation, especially under ER stress conditions (Fig. 2*A*).

In patients with Wolfram syndrome, destruction of β cells leads to juvenile-onset diabetes (25). This finding prompted us to examine whether WFS2 was also involved in pancreatic β cell death. As was seen in neuronal cells, knockdown of WFS2 in rodent β cell lines INS1 832/13 (Fig. 2*C*) and MIN6 (Fig. S2) was also associated with increased caspase-3 cleavage under both normal and ER stress conditions. The association of WFS2 with calpain 2 and their involvement in cell viability suggested that calpain 2 activation might be the cause of cell death in WFS2-deficient cells. To further explore the relationship between WFS2 and calpain 2, we expressed WFS2 together with the calpain 2 catalytic subunit CAPN2 and measured apoptosis. Ectopic expression of WFS2 significantly suppressed calpain 2-associated apoptosis under normal and ER stress conditions (Fig. 2*D*, lane 4 and lane 8, and Fig. 2*E*). Next, we tested whether CAPN2 mediates cell death induced by WFS2 deficiency. When CAPN2 was silenced in WFS2-deficient cells, apoptosis was partially suppressed compared with untreated WFS2-deficient cells (Fig. 2*F*). Taken together, these results suggest that WFS2 is a negative regulator of calpain 2 proapoptotic functions.

To further confirm that loss of function of WFS2 leads to cell death mediated by calpain 2, we tested if calpeptin, a calpain inhibitor, could prevent cell death in WFS2-deficient cells. In agreement with previous observations, calpeptin treatment prevented WFS2-knockdown-mediated cell death in neuronal (Fig. 3 *A* and *B*) and β cell lines (Fig. 3*C* and Fig. S3*A*). Collectively, these results indicate that WFS2 is a suppressor of calpain 2-mediated cell death.

CAPN2 is the catalytic subunit of calpain 2. CAPN2 forms a heterodimer with the regulatory subunit, CAPNS1, which is required for protease activity and stability. We next explored the role of WFS2 in CAPN2 and CAPNS1 protein stability. Ectopic expression or RNAi-mediated knockdown of WFS2 did not correlate with changes in the steady-state expression of CAPN2 (Fig. S3*B*). By contrast, overexpression of WFS2 significantly reduced CAPNS1 protein expression (Fig. 3*D*) and transient suppression of WFS2 slightly increased CAPNS1 protein expression (Fig. 3*D*). These data suggest that WFS2 might be involved in CAPNS1 protein turnover, which is supported by the data showing that GST-tagged WFS2 expressed in HEK293 cells associated with endogenous CAPNS1 (Fig. 1*C*). To investigate whether WFS2 regulates CAPNS1 stability through the ubiquitin-proteasome pathway, we treated HEK293 cells ectopically expressing WFS2 with a proteasome inhibitor, MG132, and then measured CAPNS1 protein level. MG132 treatment stabilized CAPNS1 protein in cells ectopically expressing WFS2 (Fig. 3*E*). Furthermore, we performed cycloheximide chase experiments using HEK293 cells ectopically expressing WFS2 and quantified CAPNS1 protein levels at different time points. Ectopic expression of WFS2 was associated with significantly accelerated CAPNS1 protein loss, indicating that WFS2 contributes to posttranslational regulation of CAPNS1 (Fig. 3*F*). To further assess whether WFS2 is involved in the ubiquitination of CAPNS1, we measured the levels of CAPNS1 ubiquitination in cells ectopically expressing WFS2 and observed that CAPNS1 ubiquitination was increased by ectopic expression of WFS2 (Fig. 3*G*).

To further investigate the role of WFS2 in calpain 2 regulation, we collected brain lysates from WFS2 knockout mice. Measured levels of cleaved spectrin, a well characterized substrate for calpain (26). Notably, protein expression levels of cleaved spectrin, as well as CAPNS1, were significantly increased in WFS2 knockout mice compared with control mice (Fig. 3*H*). Collectively, these results indicate that WFS2 inhibits calpain 2 activation by regulating CAPNS1 degradation mediated by the ubiquitin-proteasome system.

Calpain 2 is a calcium-dependent protease. *WFS1*, the other causative gene for Wolfram syndrome, has been shown to be involved in calcium homeostasis (27, 28), suggesting that the loss of function of WFS1 may also cause calpain activation. To evaluate this possibility, we measured calpain activation levels in brain tissues from WFS1 brain-specific knockout and control mice. We observed a significant increase in a calpain-specific spectrin cleavage product, reflecting higher calpain activation levels in WFS1 knockout mice compared with control mice (Fig. 4*A*). The suppression levels of WFS1 in different parts of the brain were shown in Fig. 4*B*. To further confirm that calpain is activated by the loss of WFS1, we looked for other calpain substrates in brain tissues from WFS1 knockout mice using a proteomics approach. Two-dimensional fluorescence gel electrophoresis identified 12 proteins differentially expressed between cerebellums of WFS1 knockout mice and those of control mice (Fig. 4 *C* and *D*). Among these, myelin basic protein (MBP) is a known substrate for calpain in the brain (29). We measured myelin basic protein levels in brain lysates from WFS1 knockout and control mice. Indeed, the cleavage and degradation of myelin basic protein was increased in WFS1 knockout mice relative to control mice (Fig. 4*E*).

Next, we looked for evidence of increased calpain activity in Wolfram syndrome patient cells. We created neural progenitor cells derived from induced pluripotent stem cells (iPSCs) of Wolfram syndrome patients with mutations in *WFS1*. Fibroblasts from four unaffected controls and five patients with Wolfram syndrome were transduced with four reprogramming genes (Sox2, Oct4, c-Myc, and Klf4) (30) (Table S2). We produced at least 10 iPSC clones from each control and Wolfram patient. All control- and Wolfram-iPSCs, exhibited characteristic human embryonic stem cell morphology, expressed pluripotency markers including ALP, NANOG, SOX2, SSEA4, TRA-1–81, and had a normal karyotype (Fig. 5 *A*–*F*). To create neural progenitor cells, we first formed neural aggregates from iPSCs. Neural aggregates were harvested at day 5, replated onto new plates to give rise to colonies containing neural rosette structures. At day 12, neural rosette clusters were collected, replated, and used as neural progenitor cells. Consistent with the data from WFS1 and WFS2 knockout mice, we observed that spectrin cleavage was increased in neural progenitor cells derived from Wolfram-iPSCs relative to control iPSCs, which indicates increased calpain activity (Fig. 5*G*).

Because calpain is known to be activated by high calcium, we explored the possibility that cytoplasmic calcium may be increased in patient cells by staining neural progenitor cells derived from

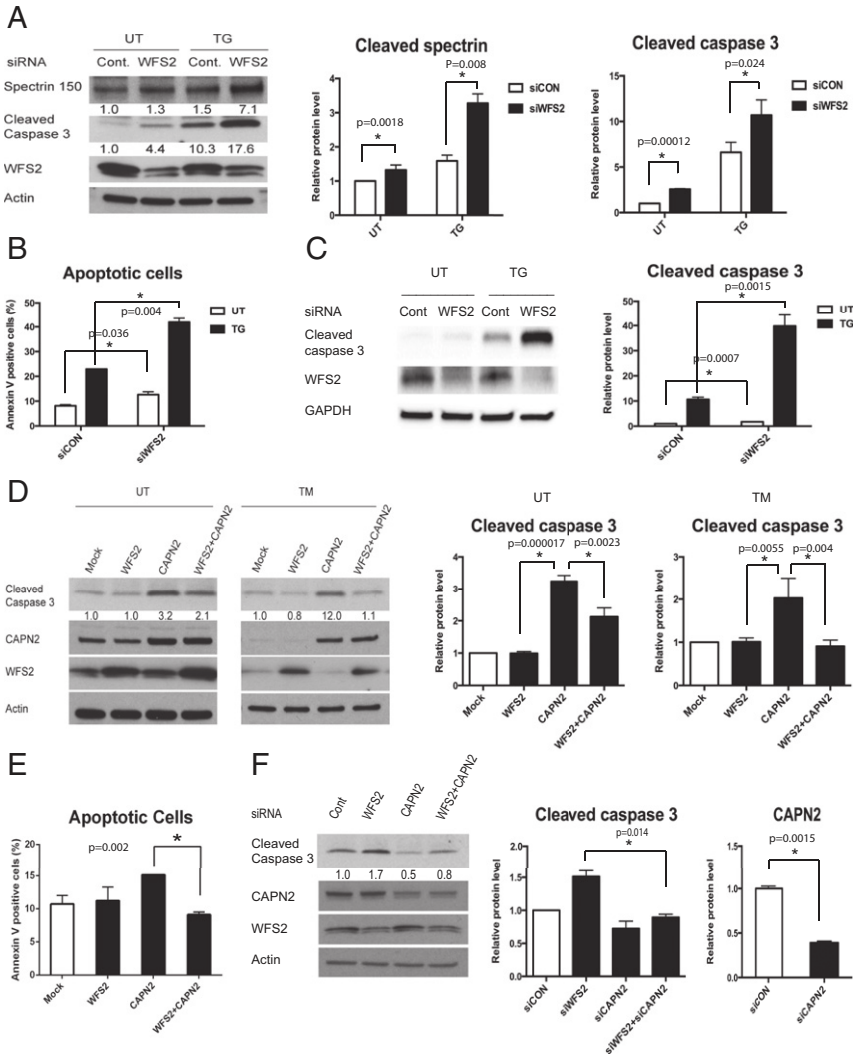

Fig. 2. WFS2 suppresses cell death mediated by CAPN2. (*A*) NSC34 cells were transfected with control scrambled siRNA or siRNA directed against WFS2, and then treated with 0.5μM thapsigargin (TG) for 6 h or untreated (UT). Apoptosis was monitored by immunoblotting analysis of cleaved caspase 3. (*Left*) Protein levels of cleaved spectrin, WFS2, and actin were measured by immunoblotting. (*Right*) Quantifications of cleaved spectrin and cleaved caspase 3 are shown ($n = 5$, $^*P < 0.05$). (*B*) NSC34 cells were transfected with control scrambled siRNA or siRNA directed against WFS2, and then treated with 0.5 μM thapsigargin (TG) for 6 h or untreated (UT). Apoptosis was monitored by Annexin V staining followed by flow cytometry analysis. ($n = 3$, $^*P < 0.05$). (*C*) INS-1 832/13 cells were transfected with control scrambled siRNA or siRNA directed against WFS2, and then treated with 0.5 μM thapsigargin (TG) for 6 h or untreated (UT). (*Left*) Expression levels of cleaved caspase 3, WFS2, and actin were measured by immunoblotting. (*Right*) Protein levels of cleaved caspase 3 are quantified ($n = 3$, $^*P < 0.05$). (*D*) NSC34 cells were transfected with empty expression plasmid (Mock), WFS2 expression plasmid, CAPN2 expression plasmid or cotransfected with WFS1 and CAPN2 expression plasmids. Twenty-four h post transfection, cells were treated with 5 μg/mL tunicamycin (TM) for 16 h or untreated (UT). Apoptosis was monitored by immunoblotting analysis of the relative levels of cleaved caspase 3 (indicated in *Left*). Expression levels of CAPN2, WFS2, and actin were also measured by immunoblotting. Quantification of cleaved caspase 3 levels under untreated (*Center*) and tunicamycin treated (*Right*) conditions are shown as bar graphs. ($n = 5$, $^*P < 0.05$). (*E*) Neuro2a cells transfected with empty expression plasmid (Mock), WFS2 expression plasmid, CAPN2 expression plasmid or cotransfected with WFS1 and CAPN2 expression plasmids were examined for apoptosis by Annexin V staining followed by flow cytometry analysis (*Right*, $n = 3$, $^*P < 0.05$). (*F*) NSC34 cells were transfected with scrambled siRNA (Cont), WFS2 siRNA, CAPN2 siRNA or cotransfected with WFS2 siRNA and CAPN2 siRNA. Apoptosis was detected by immunoblotting of cleaved caspase 3. (*Left*) Protein levels of CAPN2, WFS2 and actin were also shown. (*Right*) Quantification of immunoblotting is shown ($n = 3$, $^*P < 0.05$).

control- and Wolfram-iPSCs with Fura-2, a fluorescent calcium indicator which enables accurate measurements of cytoplasmic calcium concentrations. Fig. 5*H*, *Left*, shows that cytoplasmic calcium levels were higher in Wolfram-iPSC-derived neuronal cells relative to control cells. This result was confirmed by staining these cells with another fluorescent calcium indicator, Fluo-4 (Fig. 5*H*, *Right*). Collectively, these results indicate that loss of function of WFS1 increases cytoplasmic calcium levels, leading to calpain activation.

The results shown above argue that the pathway leading to calpain activation provides potential therapeutic targets for Wolfram syndrome. To test this concept, we elected to focus on modulating cytosolic calcium and performed a small-scale screen to identify chemical compounds that could prevent cell death mediated by thapsigargin, a known inhibitor for ER calcium ATPase. Among 73 well characterized chemical compounds that we tested (Table S3), 8 could significantly suppress thapsigargin-mediated cell death. These were PARP inhibitor, dantrolene, NS398, pioglitazone, calpain inhibitor III, docosahexaenoic acid (DHA), rapamycin, and GLP-1 (Fig. 6*A*). GLP-1, pioglitazone, and rapamycin are FDA-approved drugs and have been shown to confer protection against ER stress-mediated cell death (27, 31–33). Dantrolene is another FDA-approved drug clinically used for muscle spasticity and malignant hyperthermia (34). Previous studies

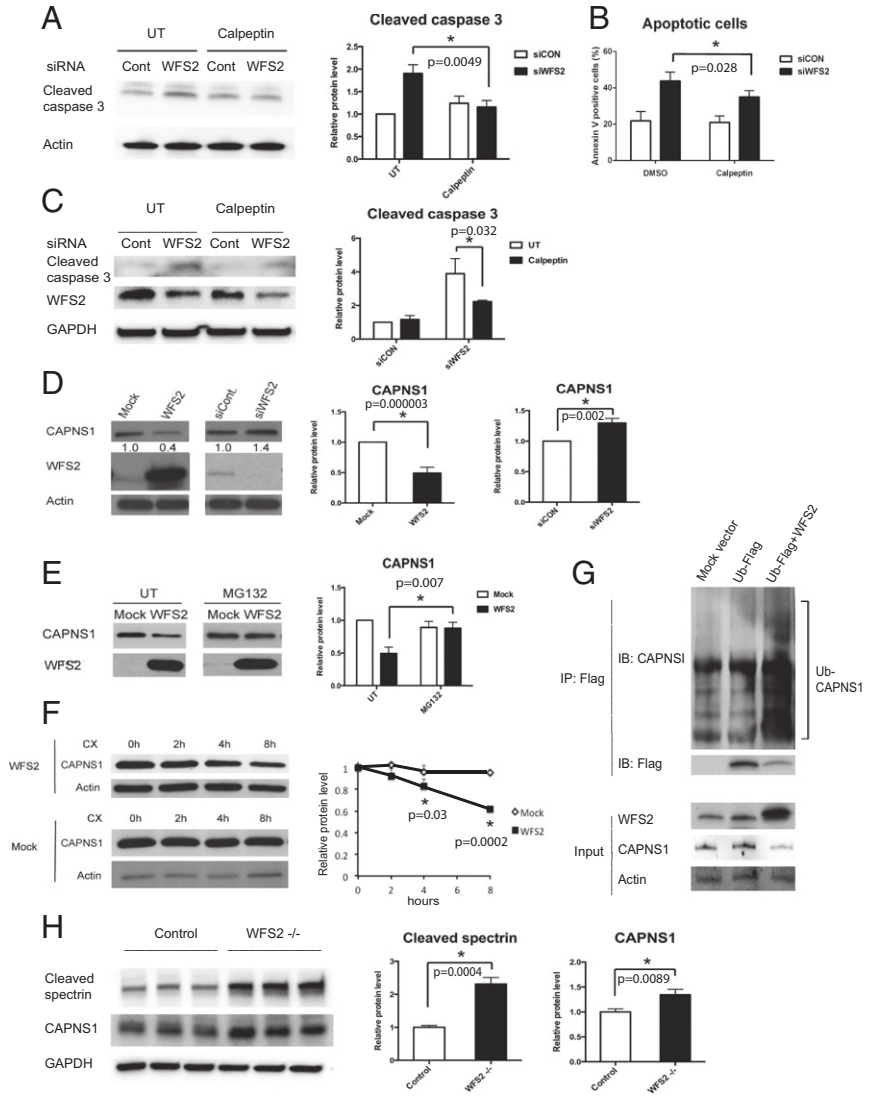

Fig. 3. WFS2 regulates calpain activity through CAPNS1. (*A*) Neuro-2a cells were transfected with siRNA against WFS2 or a control scrambled siRNA. Thirty-six h after transfection, cells were treated with or without 100μM calpeptin for 12 h. Cleaved caspase 3 and actin levels were assessed by immunoblotting (left panel). Cleaved caspase 3 protein levels are quantified in the right panel ($n = 3$, $^*P < 0.05$). (*B*) Neuro-2a cells were transfected with siRNA against WFS2 or scrambled siRNA. Thirty-six h after transfection, cells were treated with or without 100 μM calpeptin for 12 h. Early stage apoptosis was monitored by Annexin V staining followed by flow cytometry ($n = 3$, $^*P < 0.05$). (*C*) INS-1 832/13 cells were transfected with scrambled siRNA and WFS2 siRNA. Twenty-four h after transfection, cells were treated with or without 5 μM calpeptin for 24 h. Cleaved caspase 3, WFS2 and actin levels were monitored by immunoblotting (*Left*) and quantified (*Right*) ($n = 3$, $^*P < 0.05$). (*D*, *Left*) CAPNS1, WFS2, and actin levels were assessed by immunoblotting in HEK293 cells transfected with empty expression plasmid (Mock), WFS2 expression plasmid, scrambled siRNA (siCON), or WFS2 siRNA (siWFS2). (*D*, *Right*) Protein levels of CAPNS1 are quantified ($n = 5$, $^*P < 0.05$). (*E*) HEK293 cells were transfected with empty (Mock) or WFS2 expression plasmid, and then treated with MG132 (2 μM) or untreated (UT). Expression levels of CAPNS1 and WFS2 were measured by immunoblotting (*Left*) and quantified (*Right*) ($n = 4$, $^*P < 0.05$). (*F*) HEK293 cells were transfected with empty or WFS2 expression plasmid, and then treated with cycloheximide (100 μM) for indicated times. (*Left*) Expression levels of CAPNS1 and actin were measured by immunoblotting. (*Right*) Band intensities corresponding to CAPNS1 in *Left* were quantified by Image J and plotted as relative rates of the signals at 0 h ($n = 3$, $^*P < 0.05$). (*G*) NSC34 cells were transfected with mock empty vector, FLAG tagged ubiquitin (Ub-FLAG) plasmid or cotransfected with WFS2 expression plasmid and Ub-FLAG plasmid. Cell lysates were immunoprecipitated with FLAG affinity beads and analyzed for ubiquitin conjugated proteins by immunoblotting. Levels of CAPNS1 and Ub-FLAG protein were measured in the precipitates. WFS2, CAPNS1 and actin expression was monitored in the input samples. (*H*) Brain lysates from control and WFS2 knockout mice were analyzed by immunoblotting. Protein levels of cleaved spectrin and CAPNS1 were determined (*Left*) and quantified (*Center* and *Right*) (each group $n = 3$, $^*P < 0.05$).

have shown that dantrolene is an inhibitor of the ER-localized ryanodine receptors and suppresses leakage of calcium from the ER to cytosol (35, 36). We thus hypothesized that dantrolene could confer protection against cell death in Wolfram syndrome, and performed a series of experiments to investigate this possibility. We first examined whether dantrolene could decrease cytoplasmic calcium levels. As expected, dantrolene treatment decreased cytosolic calcium levels in INS-1 832/13 and NSC34 cells (Fig. S4 *A* and *B*). We next asked whether dantrolene could restore cytosolic calcium levels in WFS1-deficient cells. RNAi-mediated WFS1 knockdown increased cytosolic calcium levels relative to control cells, and dantrolene treatment restored cytosolic calcium levels in WFS1-knockdown INS-1 832/13 cells (Fig. 6*B*, *Left*) as well as WFS1-knockdown NSC34 cells (Fig. 6*B*, *Right*). Next, to determine whether dantrolene confered protection in WFS1-deficient cells, we treated WFS1 silenced INS-1 832/13 cells with dantrolene and observed suppression of apoptosis (Fig. 6*C*) and calpain activity (Fig. 6*D*). Dantrolene treatment also prevented

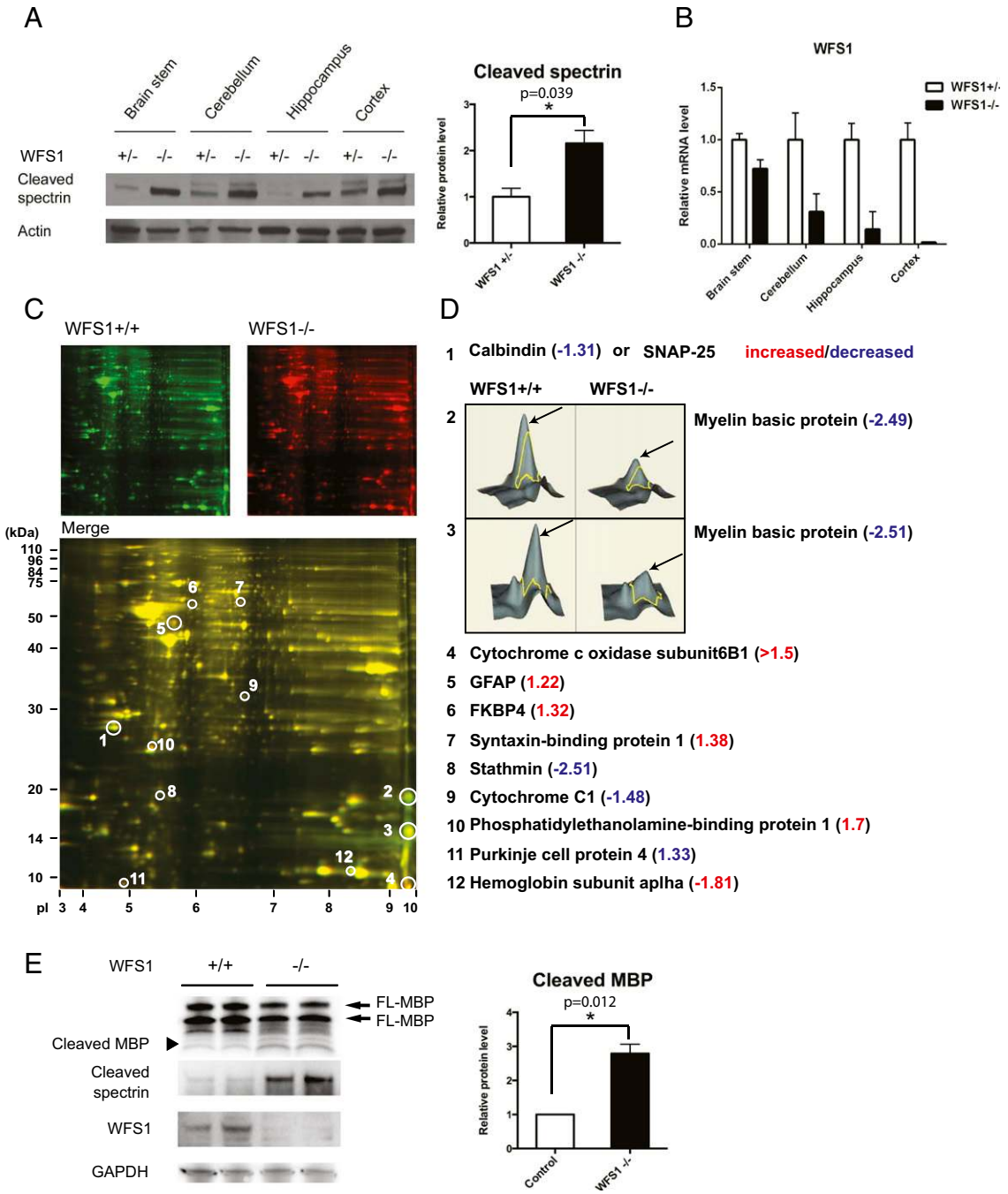

Fig. 4. Evidence of Calpain 2 activation in a mouse model of Wolfram syndrome. (*A*) Protein was extracted from brain tissues of WFS1 brain-specific knockout (–/–) and control (+/–) mice. (*Left*) Cleaved alpha II spectrin and actin levels were determined by immunoblot analysis. (*Right*) Quantification of cleaved spectrin is shown (each group $n = 10$, $^*P < 0.05$). (*B*) WFS1 mRNA levels in different parts of brain in WFS1$^{-/-}$ and WFS1$^{+/-}$ mice were measured by qRT-PCR. (*C*) Two-dimensional fluorescence difference gel electrophoresis of cerebellum proteins from WFS1 knockout (WFS1$^{-/-}$, labeled in red) and control (WFS1$^{+/+}$, labeled in green) mice showing common (Merge, labeled in yellow) and unique proteins (circled). (*D*) The protein expression ratios between WFS1 knockout and control mice were generated, and differentially expressed spots were analyzed by MALDI-TOF mass spectrometry. Quantitative diagrams of spots #2 and #3, identified by mass spectrometry as myelin basic protein, showing lower levels of expression in WFS1 knockout mice compared with control mice. (*E*) Protein was extracted from cerebellums of WFS1 brain-specific knockout (–/–) and control (+/+) mice. Cleaved myelin basic protein (black arrow), cleaved spectrin, WFS1 and GAPDH levels were determined by immunoblot analysis (left panel) and quantified in the right panel (each group $n = 3$, $^*P < 0.05$).

calpain activation and cell death in WFS1-knockdown NSC34 cells (Fig. 6*E*). To verify these observations in patient cells, we pretreated neural progenitor cells derived from iPSCs of a Wolfram syndrome patient and an unaffected parent with dantrolene, and then challenged these cells with thapisgargin. Thapsigargin-induced cell death was increased in neural progenitor cells derived from the Wolfram syndrome patient relative to those derived from the unaffected parent, and dantrolene could prevent cell death in the patient iPSC-derived neural progenitor cells (Fig. 6*F*). In addition, we treated brain-specific WFS1 knockout mice with dantrolene and observed evidence of suppressed calpain activation in brain lysates from these mice (Fig. 6*G*). Collectively, these results argue

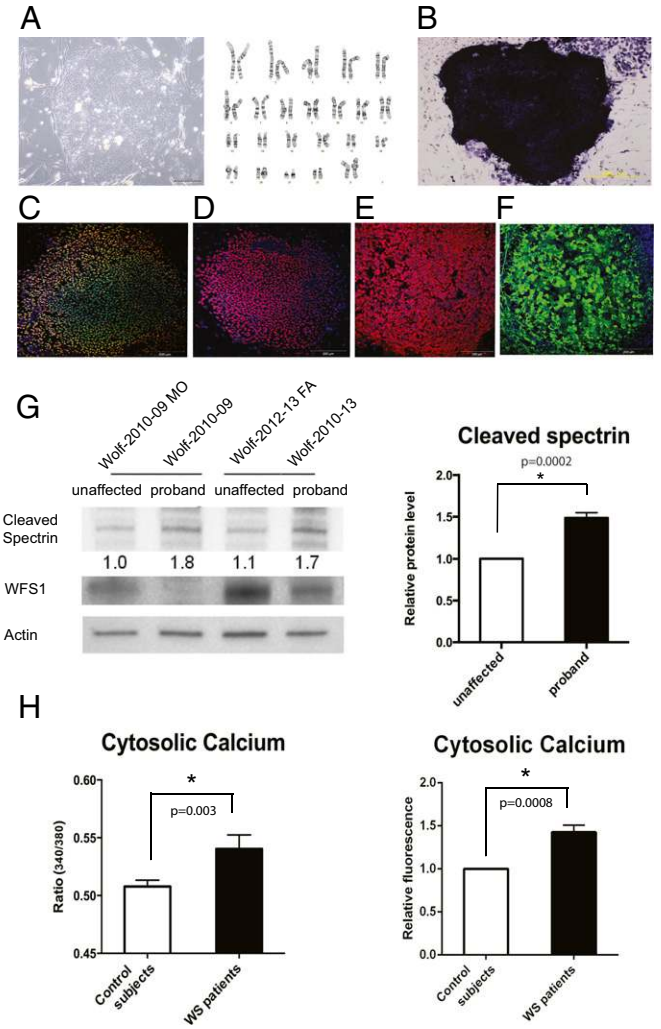

Fig. 5. High cytosolic calcium levels and hyperactivation of calpain in patient neural progenitor cells. (*A*, *Left*) Wolfram syndrome iPS cells derived from fibroblasts of a patient 1610. (*A*, *Right*) Karyotype of the Wolfram iPS cells. (*B*) Alkaline phosphatase staining of the Wolfram iPS cells. (*C*–*F*) Wolfram syndrome iPS cells stained with pluripotent markers: Nanog (*C*), Sox2 (*D*), SSEA4 (*E*), and TRA-1 (*F*). (*G*) Immunoblot analysis of cleaved spectrin and actin in neural progenitor cells derived from Wolfram syndrome patient iPS cells. The relative levels of the spectrin cleavage product are indicated (*Left*) and quantified (*Right*) ($n = 4$, $^*P < 0.05$). (*H*, *Left*) Quantitative analysis of cytosolic calcium levels in unaffected controls and Wolfram syndrome patients measured by Fura-2 calcium indicator (All values are means ± SEM; experiment was performed six independent times with >3 wells per sample each time; $n = 6$, $^*P < 0.05$). (*H*, *Right*) Quantification of cytosolic calcium levels in unaffected controls and Wolfram syndrome patients measured by Fluo-4 calcium assay (experiment was performed four independent times; $n = 4$, $^*P < 0.05$).

that dantrolene could prevent cell death in Wolfram syndrome by suppressing calpain activation.

Discussion

Growing evidence indicates that ER dysfunction triggers a range of human chronic diseases, including diabetes, atherosclerosis, inflammatory bowel disease, and neurodegenerative diseases (3, 4, 37–39). However, currently there is no effective therapy targeting the ER for such diseases due to the lack of clear understanding of the ER's contribution to the pathogenesis of these diseases. Although Wolfram syndrome is a rare disease and therefore not a focus of drug discovery efforts, the homogeneity of the patient population and disease mechanism has enabled us to identify a potential target, a calcium-dependent protease, calpain. Our results provide new insights into how the pathways leading to calpain activation cause β cell death and neurodegeneration, which are schematically summarized in Fig. 6*H*.

There are two causative genes for Wolfram syndrome, *WFS1* and *WFS2*. The functions of WFS1 have been extensively studied in pancreatic β cells. It has been shown that WFS1-deficient pancreatic β cells have high baseline ER stress levels and impaired insulin synthesis and secretion. Thus, WFS1-deficient β cells are susceptible to ER stress mediated cell death (5, 6, 32, 40–42). The functions of WFS2 are still not clear. There is evidence showing that impairment of WFS2 function can cause neural atrophy, muscular atrophy, and accelerate aging in mice (14). WFS2 has also been shown to be involved in autophagy (43). However, although patients with both genetic types of Wolfram syndrome suffer from the same disease manifestations, it was not clear if a common molecular pathway was altered in these patients. Our study has demonstrated, to our knowledge for the first time, that calpain hyperactivation is the common molecular pathway altered in patients with Wolfram syndrome. The mechanisms of calpain hyperactivation are different in the two genetic types of Wolfram syndrome. WFS1 mutations cause calpain activation by increasing cytosolic calcium levels, whereas WFS2 mutations lead to calpain activation due to impaired calpain inhibition.

Previously, Wolfram syndrome studies focused on pancreatic β cell function (5, 40, 41). However, patients also suffer from neuronal manifestations. MRI scans of Wolfram syndrome patients showed atrophy in brain tissue implying neurodegeneration in patients (7, 10). To investigate the mechanisms of neurodegeneration in Wolfram syndrome human cells, we established Wolfram syndrome iPSC-derived neural progenitor lines and confirmed the observations found in rodent cells and animal models of Wolfram syndrome. Differentiation of these iPSC-derived neural progenitor cells into specific types of neurons should be carried out in the future to better understand which cell types are damaged in Wolfram syndrome; this will lead to a better understanding of the molecular basis of this disease and provide cell models for future drug development.

Calpain activation has been found to be associated with type 2 diabetes and various neuronal diseases including Alzheimers, traumatic brain injury and cerebral ischemia, suggesting that regulation of calpains is crucial for cellular health (23). We discovered that calpain inhibitor III could confer protection against thapsigargin mediated cell death (Fig. 6*A*). Our data also demonstrates that calpeptin treatment was beneficial for cells with impaired WFS2 function. These results suggest that targeting calpain could be a novel therapeutic strategy for Wolfram syndrome. However, calpain is also an essential molecule for cell survival (44). Controlling calpain activation level is a double-bladed sword. We should carefully monitor calpain functions in treating patients with Wolfram syndrome (44).

Calpain activation is tightly regulated by cytosolic calcium levels. In other syndromes that increase cytosolic calcium level in pancreatic β cells, patients experience a transient or permanent period of hyperinsulinaemic hypoglycemia. This hyperinsulinaemic hypoglycemia can be partially restored by an inhibitor for ATP-sensitive potassium (K_{ATP}) channels or a calcium channel antagonist that prevents an increase in cytosolic calcium levels (45, 46). Although patients with Wolfram syndrome do not experience a period of hyperinsulinaemic hypoglycemia, small molecule compounds capable of altering cellular calcium levels may prevent calpain 2 activation and hold promise for treating patients with Wolfram syndrome. Treatment of WFS1-knockdown cells with dantrolene and ryanodine could prevent cell death mediated by WFS1 knockdown. Dantrolene is a muscle relaxant drug prescribed for multiple sclerosis, cerebral palsy or malignant hyperthermia (47). Dantrolene inhibits the ryanodine receptors and

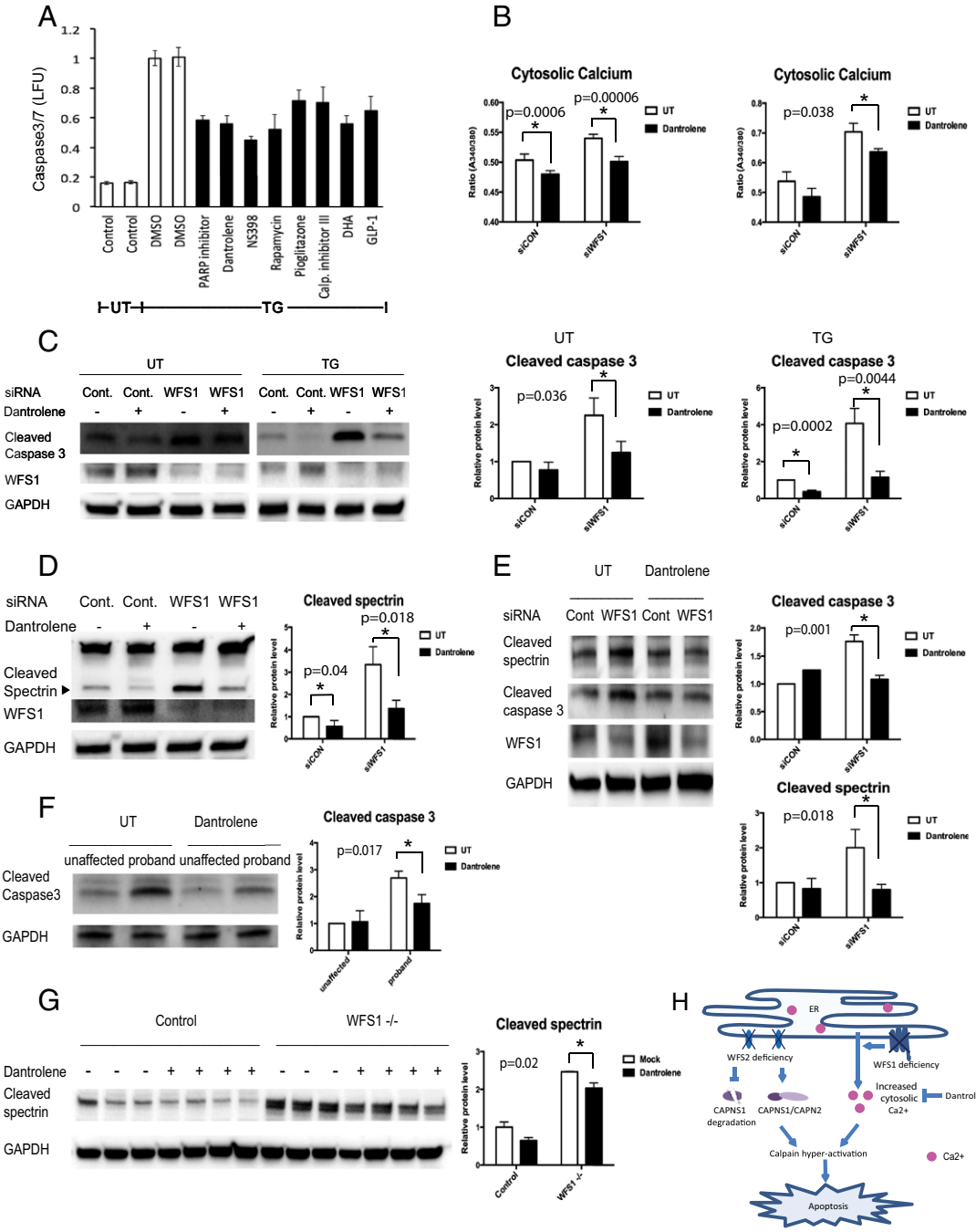

Fig. 6. Dantrolene prevents cell death in iPS cell-derived neural progenitor cells of Wolfram syndorme by inhibiting the ER calcium leakage to the cytosol. (*A*) INS-1 832/13 cells were pretreated with DMSO or drugs for 24 h then incubated in media containing 20 nM of thapsigargin (TG) overnight. Apoptosis was detected by caspase 3/7-Glo luminescence. (*B*) Cytosolic calcium levels were determined by Fura-2 in control and WFS1-deficient INS-1 832/13 (*Left*) and NSC34 (*Right*) cells treated or untreated with 10 μM dantrolene for 24 h (*All* values are means ± SEM; experiment was performed 6 independent times with >3 wells per sample each time $n = 6$, $^*P < 0.05$). (*C*) INS-1 832/13 cells were transfected with scrambled siRNA or siRNA against WFS1. Cells were pretreated with or without 10 μM dantrolene for 48 h, then incubated in media with or without 0.5 μM TG for 6 h. Expression levels of cleaved caspase-3, WFS1, GAPDH were measured by immunoblotting (*Left*). Protein levels of caspase3 under untreated (*Center*) and TG treated (*Right*) conditions are quantified and shown as bar graphs ($n = 3$, $^*P < 0.05$). (*D*) INS-1 832/13 cells were transfected with scrambled siRNA or siRNA against WFS1, pretreated with or without 10 μM dantrolene for 48 h, then incubated in media containing 0.5 μM TG for 6 h. Protein levels of cleaved spectrin, WFS1, GAPDH were analyzed by immunoblotting (*Left*) and quantified (*Right*) ($n = 3$, $^*P < 0.05$). (*E*) NSC34 cells were transfected with scrambled siRNA or siRNA against WFS1. Then treated with or without10 μM dantrolene for 24 h. Protein levels of cleaved spectrin, cleaved caspase 3, WFS2 and GAPDH were determined by immunoblotting (*Left*) and quantified (*Right*) ($n = 3$, $^*P < 0.05$). (*F*) Wolfram patient neural progenitor cells were pretreated with or without 10 μM dantrolene for 48 h. Then, cells were treated with 0.125 μM TG for 20 h. (*Left*) Apoptosis was monitored by immunoblotting. (*Right*) Quantification of cleaved caspase 3 protein levels are indicated ($n = 3$, $^*P < 0.05$). (*G*) Control and WFS1 brain-specific knockout mice were treated with water or dantrolene for 4 wk at 20 mg/kg. Brain lysates of these mice were examined by immunoblotting. Protein levels of cleaved spectrin and GAPDH were monitored (*Left*) and quantified (*Right*) (All values are means ± SEM; each group $n > 3$, $^*P < 0.05$). (*H*) Scheme of the pathogenesis of Wolfram syndrome.

reduces calcium leakage from the ER to cytosol, lowering cytosolic calcium level. The protective effect of dantrolene treatment on WFS1-deficient cells suggests that dysregulated cellular calcium homeostasis plays a role in the disease progression of Wolfram syndrome. In addition, it has been shown that stabilizing ER calcium channel function could prevent the progression of neurodegeneration in a mouse model of Alzheimer's disease (48). Therefore, modulating calcium levels may be an effective way to treat Wolfram syndrome or other ER diseases.

Dantrolene treatment did not block cell death mediated by WFS2 knockdown, suggesting that WFS2 does not directly affect the ER calcium homeostasis (Fig. S4 *D* and *E*). RNAi-mediated WFS1 knockdown in HEK293 cells significantly reduced the activation levels of sarco/endoplasmic reticulum calcium transport ATPase (SERCA), indicating that WFS1 may play a role in the modulation of SERCA activation and ER calcium levels (Fig. S5). It has been shown that WFS1 interacts with the Na^+/K^+ ATPase β1 subunit and the expression of WFS1 parallels that of Na^+/K^+ ATPase β1 subunit in a variety of settings, suggesting that WFS1 may function as an ion channel or regulator of existing channels (42). Further studies on this topic would be necessary to completely understand the etiology of Wolfram syndrome.

Our study reveals that dantrolene can prevent ER stress-mediated cell death in human and rodent cell models as well as mouse models of Wolfram syndrome. Thus, dantrolene and other drugs that regulate ER calcium homeostasis could be used to delay the progression of Wolfram syndrome and other diseases associated with ER dysfunction, including type 1 and type 2 diabetes.

Materials and Methods

Human Subjects. Wolfram syndrome patients were recruited through the Washington University Wolfram Syndrome International Registry website (wolframsyndrome.dom.wustl.edu). The clinic protocol was approved by the Washington University Human Research Protection Office and all subjects provided informed consent if adults and assent with consent by parents if minor children (IRB ID 201107067 and 201104010).

Animal Experiments. WFS1 brain-specific knockout mice were generated by breeding the Nestin-Cre transgenic mice (Jackson Laboratory) with WFS1 floxed mice (40). WFS2 whole body knockout mice are purchased from MRC Harwell. All animal experiments were performed according to procedures approved by the Institutional Animal Care and Use Committee at the Washington University School of Medicine (A-3381-01).

Calcium Levels. Calcium levels in cells were measured by Fura-2 AM dye and Fluo-4 AM dye (Life Technology) Inifinite M1000 (Tecan). Cells were plated in 96-well plates at 25,000 cells per well and stained with 4 μg/mL Fura-2 dye along with 2.5 mM probenecid for 30 min, then the cells were washed with PBS and kept in the dark for another 30 min to allow cleavage of AM ester. Fluorescence was measured at excitation wavelength 510 nm and emission wavelengths 340 nm and 380 nm. Then background subtractions were performed with both emission wavelengths. The subtraction result was used to calculate 340/380 ratios.

For Fluo-4 AM staining, neural progenitor cells were plated in 24-well plates at 200,000 cells per well. After staining with Fluo-4 AM dye for 30 min along with 2.5 mM probenecid, cells were washed and resuspended in PBS. Incubation for a further 30 min was performed to allow complete deesterification of intracellular AM esters. Then, samples were measured by flow cytometry at the FACS core facility of Washington University School of Medicine using a LSRII instrument (BD). The results were analyzed by FlowJo ver.7.6.3.

Statistical Analysis. Two-tailed *t* tests were used to compare the two treatments. *P* values below 0.05 were considered significant. All values are shown as means ± SD if not stated. Please see *SI Materials and Methods* for complete details.

ACKNOWLEDGMENTS. We thank all of the participants in the Washington University Wolfram Registry and Clinic and their families for their time and effort (wolframsyndrome.dom.wustl.edu/). We also thank Mai Kanekura, Mariko Hara, and Karen Sargent for technical support and the Washington University Wolfram Study Group Members and the study staff for advice and support in the greater research program. This work was supported by NIH Grants DK067493, P60 DK020579, and UL1 TR000448; Juvenile Diabetes Research Foundation Grants 47-2012-760 and 17-2013-512; American Diabetes Association Grant 1-12-CT-61, the Team Alejandro, The Team Ian, the Ellie White Foundation for Rare Genetic Disorders, and the Jack and J. T. Snow Scientific Research Foundation (F.U.).

1. Ron D, Walter P (2007) Signal integration in the endoplasmic reticulum unfolded protein response. *Nat Rev Mol Cell Biol* 8(7):519–529.
2. Tabas I, Ron D (2011) Integrating the mechanisms of apoptosis induced by endoplasmic reticulum stress. *Nat Cell Biol* 13(3):184–190.
3. Hetz C, Chevet E, Harding HP (2013) Targeting the unfolded protein response in disease. *Nat Rev Drug Discov* 12(9):703–719.
4. Wang S, Kaufman RJ (2012) The impact of the unfolded protein response on human disease. *J Cell Biol* 197(7):857–867.
5. Fonseca SG, et al. (2005) WFS1 is a novel component of the unfolded protein response and maintains homeostasis of the endoplasmic reticulum in pancreatic beta-cells. *J Biol Chem* 280(47):39609–39615.
6. Fonseca SG, et al. (2010) Wolfram syndrome 1 gene negatively regulates ER stress signaling in rodent and human cells. *J Clin Invest* 120(3):744–755.
7. Barrett TG, Bundey SE, Macleod AF (1995) Neurodegeneration and diabetes: UK nationwide study of Wolfram (DIDMOAD) syndrome. *Lancet* 346(8988):1458–1463.
8. Wolfram DJ, Wagener HP (1938) Diabetes mellitus and simple optic atrophy among siblings: Report of four cases. *Mayo Clin Proc* 1:715–718.
9. Urano F (2014) Diabetes: Targeting endoplasmic reticulum to combat juvenile diabetes. *Nat Rev Endocrinol* 10(3):129–130.
10. Hershey T, et al.; Washington University Wolfram Study Group (2012) Early brain vulnerability in Wolfram syndrome. *PLoS ONE* 7(7):e40604.
11. Marshall BA, et al.; Washington University Wolfram Study Group (2013) Phenotypic characteristics of early Wolfram syndrome. *Orphanet J Rare Dis* 8(1):64.
12. Inoue H, et al. (1998) A gene encoding a transmembrane protein is mutated in patients with diabetes mellitus and optic atrophy (Wolfram syndrome). *Nat Genet* 20(2):143–148.
13. Amr S, et al. (2007) A homozygous mutation in a novel zinc-finger protein, ERIS, is responsible for Wolfram syndrome 2. *Am J Hum Genet* 81(4):673–683.
14. Chen YF, et al. (2009) Cisd2 deficiency drives premature aging and causes mitochondria-mediated defects in mice. *Genes Dev* 23(10):1183–1194.
15. Wiley SE, et al. (2013) Wolfram Syndrome protein, Miner1, regulates sulphydryl redox status, the unfolded protein response, and Ca2+ homeostasis. *EMBO Mol Med* 5(6):904–918.
16. Shang L, et al. (2014) β-cell dysfunction due to increased ER stress in a stem cell model of Wolfram syndrome. *Diabetes* 63(3):923–933.
17. Sandhu MS, et al. (2007) Common variants in WFS1 confer risk of type 2 diabetes. *Nat Genet* 39(8):951–953.
18. Bonnycastle LL, et al. (2013) Autosomal dominant diabetes arising from a Wolfram syndrome 1 mutation. *Diabetes* 62(11):3943–3950.
19. Goll DE, Thompson VF, Li H, Wei W, Cong J (2003) The calpain system. *Physiol Rev* 83(3):731–801.
20. Tan Y, et al. (2006) Ubiquitous calpains promote caspase-12 and JNK activation during endoplasmic reticulum stress-induced apoptosis. *J Biol Chem* 281(23):16016–16024.
21. Tan Y, Wu C, De Veyra T, Greer PA (2006) Ubiquitous calpains promote both apoptosis and survival signals in response to different cell death stimuli. *J Biol Chem* 281(26):17689–17698.
22. Nakagawa T, Yuan J (2000) Cross-talk between two cysteine protease families. Activation of caspase-12 by calpain in apoptosis. *J Cell Biol* 150(4):887–894.
23. Cui W, et al. (2013) Free fatty acid induces endoplasmic reticulum stress and apoptosis of β-cells by Ca2+/calpain-2 pathways. *PLoS ONE* 8(3):e59921.
24. Huang CJ, et al. (2010) Calcium-activated calpain-2 is a mediator of beta cell dysfunction and apoptosis in type 2 diabetes. *J Biol Chem* 285(1):339–348.
25. Barrett TG, Bundey SE (1997) Wolfram (DIDMOAD) syndrome. *J Med Genet* 34(10):838–841.
26. Liu MC, et al. (2006) Comparing calpain- and caspase-3-mediated degradation patterns in traumatic brain injury by differential proteome analysis. *Biochem J* 394(Pt 3):715–725.
27. Hara T, et al. (2014) Calcium efflux from the endoplasmic reticulum leads to β-cell death. *Endocrinology* 155(3):758–768.
28. Takei D, et al. (2006) WFS1 protein modulates the free Ca(2+) concentration in the endoplasmic reticulum. *FEBS Lett* 580(24):5635–5640.
29. Liu MC, et al. (2006) Extensive degradation of myelin basic protein isoforms by calpain following traumatic brain injury. *J Neurochem* 98(3):700–712.
30. Takahashi K, Yamanaka S (2006) Induction of pluripotent stem cells from mouse embryonic and adult fibroblast cultures by defined factors. *Cell* 126(4):663–676.
31. Yusta B, et al. (2006) GLP-1 receptor activation improves beta cell function and survival following induction of endoplasmic reticulum stress. *Cell Metab* 4(5):391–406.
32. Akiyama M, et al. (2009) Increased insulin demand promotes while pioglitazone prevents pancreatic beta cell apoptosis in Wfs1 knockout mice. *Diabetologia* 52(4):653–663.
33. Bachar-Wikstrom E, et al. (2013) Stimulation of autophagy improves endoplasmic reticulum stress-induced diabetes. *Diabetes* 62(4):1227–1237.
34. Dykes MH (1975) Evaluation of a muscle relaxant: Dantrolene sodium (Dantrium). *JAMA* 231(8):862–864.

35. Wei H, Perry DC (1996) Dantrolene is cytoprotective in two models of neuronal cell death. *J Neurochem* 67(6):2390–2398.
36. Luciani DS, et al. (2009) Roles of IP3R and RyR Ca2+ channels in endoplasmic reticulum stress and beta-cell death. *Diabetes* 58(2):422–432.
37. Hotamisligil GS (2010) Endoplasmic reticulum stress and atherosclerosis. *Nat Med* 16(4):396–399.
38. Hotamisligil GS (2010) Endoplasmic reticulum stress and the inflammatory basis of metabolic disease. *Cell* 140(6):900–917.
39. Ozcan L, Tabas I (2012) Role of endoplasmic reticulum stress in metabolic disease and other disorders. *Annu Rev Med* 63:317–328.
40. Riggs AC, et al. (2005) Mice conditionally lacking the Wolfram gene in pancreatic islet beta cells exhibit diabetes as a result of enhanced endoplasmic reticulum stress and apoptosis. *Diabetologia* 48(11):2313–2321.
41. Ishihara H, et al. (2004) Disruption of the WFS1 gene in mice causes progressive beta-cell loss and impaired stimulus-secretion coupling in insulin secretion. *Hum Mol Genet* 13(11):1159–1170.
42. Zatyka M, et al. (2008) Sodium-potassium ATPase 1 subunit is a molecular partner of Wolframin, an endoplasmic reticulum protein involved in ER stress. *Hum Mol Genet* 17(2):190–200.
43. Chang NC, Nguyen M, Germain M, Shore GC (2010) Antagonism of Beclin 1-dependent autophagy by BCL-2 at the endoplasmic reticulum requires NAF-1. *EMBO J* 29(3): 606–618.
44. Dutt P, et al. (2006) m-Calpain is required for preimplantation embryonic development in mice. *BMC Dev Biol* 6:3.
45. Arya VB, Mohammed Z, Blankenstein O, De Lonlay P, Hussain K (2014) Hyperinsulinaemic hypoglycaemia. *Hormone Metabolic Res* 46(3):157–170.
46. Shah P, Demirbilek H, Hussain K (2014) Persistent hyperinsulinaemic hypoglycaemia in infancy. *Semin Pediatr Surg* 23(2):76–82.
47. Krause T, Gerbershagen MU, Fiege M, Weisshorn R, Wappler F (2004) Dantrolene—a review of its pharmacology, therapeutic use and new developments. *Anaesthesia* 59(4):364–373.
48. Chakroborty S, et al. (2012) Stabilizing ER Ca2+ channel function as an early preventative strategy for Alzheimer's disease. *PLoS ONE* 7(12):e52056.

Supporting Information

Lu et al. 10.1073/pnas.1421055111

SI Materials and Methods

Reagents. Thapsigargin, tunicamycin, calpeptin dantrolene, ryanodine, and cycloheximide were obtained from SIGMA. RPMI-1640 and DMEM were from Invitrogen. Neural induction media, neural proliferation media were from Stemcell Technologies. MitoProbe DilC1(5) mitochondrial membrane potential assay kit, Annexin V Alexa Flour488 conjugate, Fluo-4, and Fura-2 calcium indicators were obtained from Invitrogen. Caspase-glo 3/7 protease assay kit and calpain-glo protease assay kit was purchased from Promega. Mito Stress test kit was from Seahorse Bioscience. Anti-WFS2 antibody, and anti-WFS1 antibody were purchased from Proteintech, anti-Caspase 3, anti-CAPN2 antibodies were obtained from Cell Signaling Technology, anti-CAPNS1 and anti-alpha II spectrin antibody were obtained from Millipore. Anti-actin antibody was purchased from SIGMA. Anti-Myelin basic protein antibody was from Santa Cruz Biotechnology. Anti-Calpain 2 antibody, which detects both CAPN2 and CAPNS1, was raised in rabbits against bacterially expressed rat calpain 2.

Plasmids and siRNA. pCMV-SPORT6-WFS2 expression plasmid was purchased from Open Biosystems. pDsRed2-ER vector was purchased from Clontech. FLAG-tagged WFS2 plasmids were constructed by inserting FLAG sequences into the N and C termini of the expression plasmid. GST-WFS2 plasmid was generated by inserting WFS2 sequence into pEBG mammalian expression plasmid. A CAPN2 expression plasmid was generated in pLenti-CMV-puro plasmid provided by E. Campeau (1). Lipofectamine2000 (Invitrogen) was used to transfect small interfering RNA (siRNA) directed against WFS2 and CAPN2 into cells. siRNAs were designed and synthesized at QIAGEN as follows: mouse WFS2 CAACAGAAGGAUAGCUUG, human WFS2 CGAAAGUAGUGAAUGAAA, human CAPN2 CCGAGGAGGUUGAAAGUA, rat WFS1 GUUUGACCGCUACAAGUUU. Cells were incubated in media overnight after siRNA transfection, and then additional treatments were performed, including ER stress induction.

Cell Culture. Neuro-2a, NSC34, HEK293, MEFs, and COS7 cells were cultured in DMEM containing 10% (vol/vol) FBS and penicillin and streptomycin. MIN6 cells were grown in DMEM containing 15% FBS and penicillin and streptomycin. INS-1 832/13 cells were cultured in RPMI containing 10% FBS before measurement. Neural progenitor cells were maintained in STEMdiff Neural Progenitor Medium from Stemcell Technologies.

iPS Cell and Neural Progenitor Cell Generation. To generate iPS cells, we obtained fibroblasts from nonaffected controls and patients with Wolfram syndrome. Integration-free iPS cells were generated via Sendai viral delivery of the four reprogramming factors, Oct4, Sox2, Klf4, and c-Myc using Life Technologies' Cytotune reagents and protocol. All WFS- and control-iPSCs showed silencing of the four transgenes, exhibited characteristic human embryonic stem cell morphology, expressed pluripotency markers including ALP, NANOG, SOX2, SSEA4, and TRA-1-81, and had a normal karyotype. To generate neural progenitor cells, iPSCs were counted and plated ~50,000 per well in a 96-well plate to form uniform embryoid bodies. After 5 d, embryoid bodies were suspended in neural induction media and replated as adherent cultures. Fresh media were applied every day for 7 d. Neural rosettes formed in these cultures were selected and plated. Plated rosettes were fed with neural induction media every day for 4–7 d to obtain neural progenitor cells.

MALDI-TOF Mass Spectrometry. HEK293 cells were transfected with GST-WFS2 plasmid and empty GST plasmid. Cell lysates were collected and immunoprecipitated with glutathione beads in lysis buffer (150 mM NaCl, 0.5% Triton X-100, 50 mM Hepes, 1 mM EDTA, 1 mM DTT, pH 7.5). The precipitated proteins from both samples were resolved by SDS/PAGE and stained with Coomassie blue staining. The distinct bands that only appear in GST-WFS2 lane but not GST lane were analyzed by MALDI-TOF tandem mass spectrometry on a Shimadzu Axima TOF2 mass spectrometry at University of Massachusetts Medical School Proteomics and mass spectrometry facility.

Immunostaining. Cells were fixed in 4% paraformaldehyde for 30 min at room temperature and then permeabilized with 0.1% Triton X-100 for 2 min. The fixed cells were washed with PBS/Tween 0.1%, blocked with Image-It FX signal enhancer (Invitrogen) for 1 h, and incubated in primary antibody overnight at 4 °C. The cells were washed three times in PBS/Tween 0.1% and incubated with secondary antibody for 1 h at room temperature. Images were obtained with a Zeiss LSM 5 PASCAL confocal microscope with LSM Image software.

FACS Analyses. For flow cytometry analyses, neural progenitor cells or NSC34 cells were plated in 24-well plates. After staining, cells were washed and resuspended in PBS. Flow cytometry analyses were performed with LSRII (BD) at the FACS core facility of Washington University School of Medicine. The results were analyzed by FlowJo ver.7.6.3.

Quantitative Real-Time PCR. Total RNA was extracted by RNeasy kits (Qiagen). Reverse transcriptase PCR was performed using High capacity reverse transcription kit (Applied Biosystems) and quantitative PCR was demonstrated with Applied Biosystems ViiA7 using SYBR green dye.

2D Fluorescence Difference Gel Electrophoresis. Proteins were extracted from cerebellums from WFS1 knockout mice and control mice. Equal amount of protein extract from paired samples were labeled by CyDye DIGE fluors. The spectrally resolvable dyes enabled simultaneous coseparation and analysis of samples on a single multiplexed gel. These paired samples were simultaneously separated on a single 2D gel, using isoelectric focusing (IEF) in the first dimension and SDS polyacrylamide gel electrophoresis (SDS/PAGE) in the second dimension. After electrophoresis, the gel was scanned using a Typhoon image scanner. Each scan revealed one of the CyDye signals (Cy3 and Cy5). ImageQuant software was used to generate the image presentation data including the single and overlay images. The comparative analysis of all spots was done by the DeCyder analysis software. The protein expression ratios between WFS1 knockout and control mice were generated, and differentially expressed spots were analyzed by MALDI-TOF mass spectrometry.

SERCA Activity Assay. The SERCA activity assay was performed as described in ref. 2. HEK293 cells were homogenized in hypotonic buffer, consisting of 10 mM $NaHCO_3$, 250 mM sucrose, 5 mM NaN_3, and 0.1 mM PMSF. ER fractions were isolated using differential centrifugation. 125–300 μg of ER protein fractions were added to the assay mixture [100 mM KCL, 30 mM imidazole-histidine (pH 6.8), 5 mM $MgCl_2$, 5 mM ATP, 5 mM $(COOK)_2$, 5 mM NaN_3, and 50 μM $CaCl_2$ (10 μCi/μmol[^{45}Ca]; $CaCl_2$ American Radiolabeled Chemicals)] heated to 37 °C for 15 min. (The amount of protein we used in this study was 125 μg per sample). The reaction was stopped by the addition of 250 mM KCl and 1 mM

$LaCl_3$. The mix was then vacuum filtered through a 0.2-μm HT Tuffryn membrane (Sigma). SERCA-dependent calcium transport was measured by comparing calcium transport in the presence or absence of 10 μM thapsigargin, a SERCA inhibitor.

1. Campeau E, et al. (2009) A versatile viral system for expression and depletion of proteins in mammalian cells. *PLoS ONE* 4(8):e6529.

2. Funai K, et al. (2013) Muscle lipogenesis balances insulin sensitivity and strength through calcium signaling. *J Clin Invest* 123(3):1229–1240.

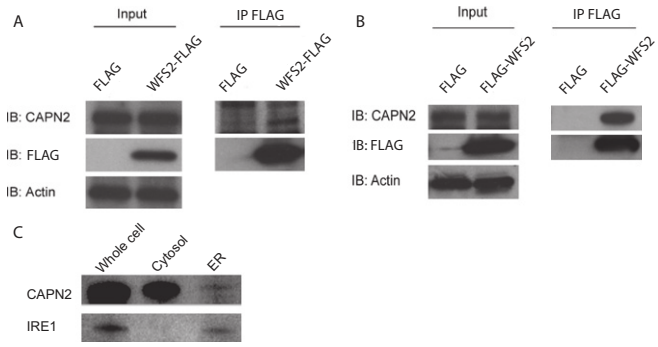

Fig. S1. FLAG-tagged WFS2 was immunoprecipitated from HEK293 cells transfected with WFS2 expression plasmids with either an N-terminal (*A*) or a C-terminal FLAG-tag (*B*), and the immunoprecipitates were analyzed for CAPN2 by immunoblotting with anti-CAPN2 antibody. (*C*) Cells were fractionated into cytosolic and ER fractions. Localization of CAPN2 and IRE1 were determined by immunoblotting.

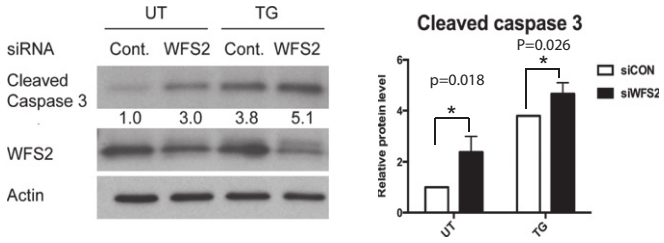

Fig. S2. MIN6 cells were transfected with control scrambled siRNA (Cont) or siRNA directed against WFS2, and then treated with 0.5 μM thapsigargin (TG) for 6 h or untreated (UT). Expression levels of cleaved caspase 3, WFS2, and actin were measured by immunoblotting (*Left*). (*Right*) Quantification of cleaved caspase 3 is indicated ($n = 3$, $^*P < 0.05$).

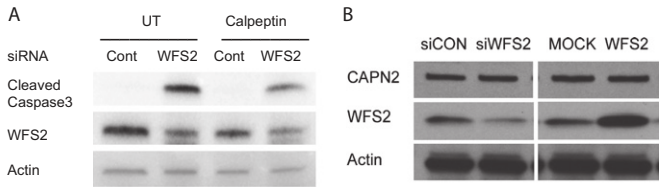

Fig. S3. (*A*) MIN6 cells were transfected with scrambled siRNA (Cont) or WFS2 siRNA. Thirty-six h after transfection, cells were treated with or without 100 μM calpeptin for 12 h. Cleaved caspase 3, WFS2, and actin levels were monitored by immunoblotting. (*B*) CAPN2, WFS2 and actin levels were assessed by immunoblotting in HEK293 cells transfected with scrambled siRNA (siCON), WFS2 siRNA (siWFS2), empty expression plasmid (Mock), or WFS2 expression plasmid (WFS2).

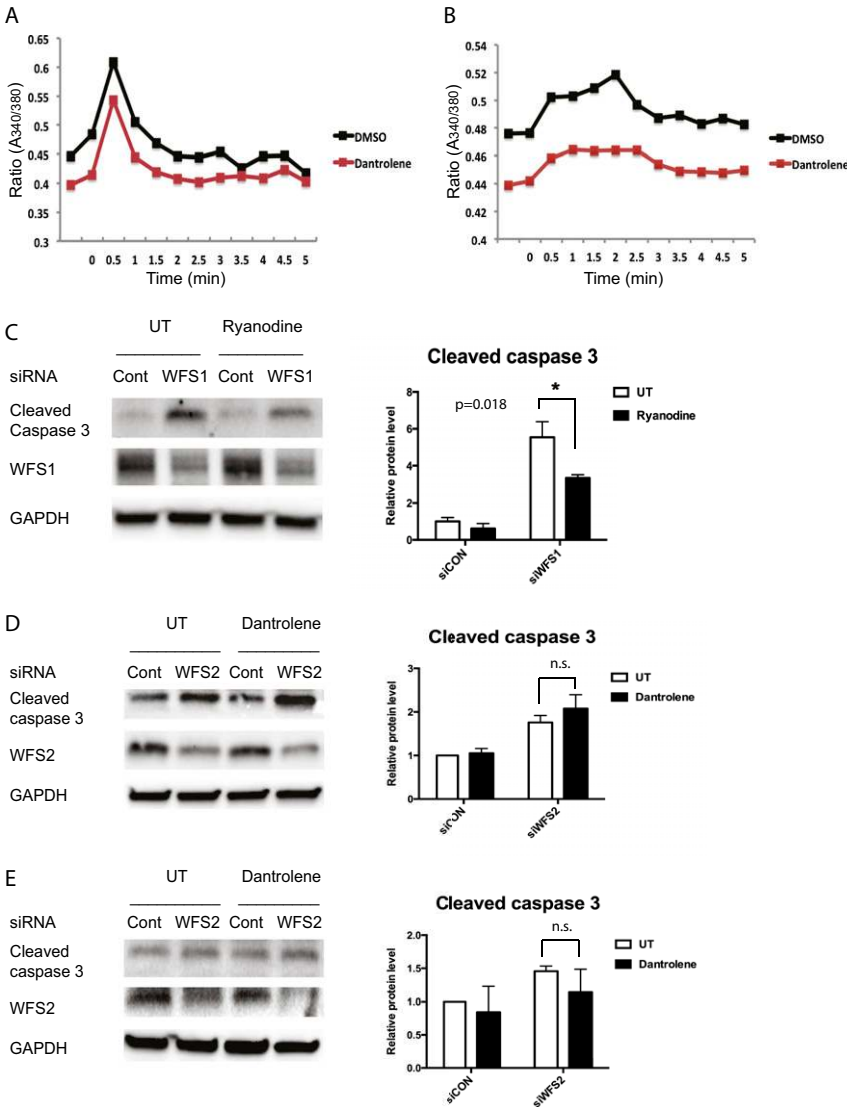

Fig. S4. INS-1 832/13 (*A*) and NSC34 (*B*) cells were pretreated with or without 10 μM dantrolene for 24 h. Cytoplasmic calcium levels were measured by Fura-2 calcium indicator over a period. Thapsigargin was added at 0 min time point ($n = 6$, the experiment was repeated six independent times). (*C*) INS-1 832/13 cells were transfected with scrambled siRNA (Cont) or WFS1 siRNA. Twenty-four h after transfection, cells were treated with or without 2 μM ryanodine for 24 h. Cleaved caspase 3, WFS1, and GAPDH levels were monitored by immunoblotting (*Left*) and quantified (*Right*) ($n = 3$, $^*P < 0.05$). (*D* and *E*) INS-1 832/13 cells (*D*) and NSC34 cells (*E*) were transfected with scrambled siRNA (Cont) and WFS2 siRNA. Twenty-four h after transfection, cells were treated with or without 10 μM dantrolene for 24 h. Cleaved caspase 3, WFS2 and GAPDH levels were monitored by immunoblotting. Quantification of cleaved caspase 3 protein levels are shown to the right ($n = 3$, $^*P < 0.05$).

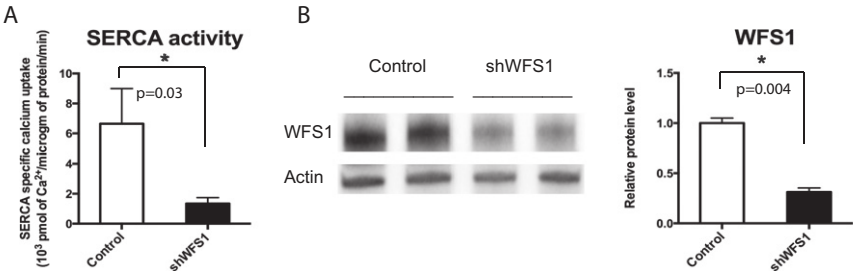

Fig. S5. (*A*) SERCA activity was measured in HEK293 cells stably expressing shRNA directed WFS1 or a scrambled sequence (Control). All values are means ± SEM. For the wild-type condition, $n = 6$; the experiment was repeated six independent times. For the WFS1 knockdown condition, $n = 7$; the experiment was repeated seven independent times. $^*P < 0.05$. (*B*) Protein levels of WFS1 and actin were monitored in HEK293 cells stably expressing shRNA directed against WFS1 or a scrambled shRNA (Control). Quantification is shown on the right ($n = 3$, $^*P < 0.05$).

Table S1. GST-WFS2 interacting proteins

Order on gel	Gene symbol	Full name	Molecular weight, KDa
1	PRKDC	DNA dependent protein kinase catalytic subunit	450
2	COPA	Coatomer Subunit alpha	140
3	IPO7, 4, 9	Importin 7, 4, and 9	120
4	XPO1, 2	Exportin 1, 2	110
5	MMS19	MMS19 nucleotide excision repair	110
6	CNX	Calnexinp	67
7	CAPN2	calpain-2	80
8	GRP78	GRP78	78
9	TUBA TUBB	Alpha and Beta Tubulin	50

Table S2. Information on genotypes and phenotypes of Wolfram syndrome and control subjects

iPSC line	Source	Clinical diagnosis	WFS1 mutation	Sex	Age at biopsy	Age at onset of DM	Age at onset of OA	Deafness	DI
Wolf-2010–5	Washington University Wolfram Clinic	WFS	H313Y	F	15	3.8	12	1.7	NA
Wolf-2010–9	Washington University Wolfram Clinic	WFS	A126T; W613X	M	16	10.8	11	NA	14
Wolf-2010–11	Washington University Wolfram Clinic	WFS	A126T; W613X	M	10	7.5	6	8	10
Wolf-2010–13	Washington University Wolfram Clinic	WFS	L200fs286Stop; E752Stop	F	7	4.8	5.2	6	7.5
GM01610	Corriell Research Institute	WFS	W648X; G695V	F	11	NA	NA	NA	NA
BJ CRL-2522	ATCC	Control	NA	M	Newborn	NA	NA	NA	NA
Wolf-2010–5-MO	Washington University Wolfram Clinic	Control	None identified	F	41	NA	NA	No	No
Wolf-2010–9 MO	Washington University Wolfram Clinic	Control	NA	F	33	NA	NA	No	No
Wolf-2012–13-FA	Washington University Wolfram Clinic	Control	NA	M	42	NA	NA	No	No

WFS, Wolfram syndrome; DM, diabetes mellitus; OA, optic atrophy; DI, diabetes insipidus.

Table S3. Chemical compounds used for a screen targeting the ER calcium homeostasis

	Drugs	Treatment conc.
1	Nicotinamide(Vitamin B3)	10 μM
2	Valproic acid	10 μM
3	Sodium tauroursodeoxycholate(TUDCA)	10 μM
4	(-)-Riboflavin(Vitamin B2,Vitamin G)	10 μM
5	Thiamine hydrochloride(Vitamin B1 hydrochloride)	10 μM
6	Memantine hydrochloride	10 μM
7	(+-)-a-Lipoic acid	10 μM
8	Kynurenic acid	10 μM
9	Folic acid	10 μM
10	Idebenone	10 μM
11	Acetovanillone(Apocynin)	10 μM
12	Aspirin	10 μM
13	Pyridoxine hydrochloride	10 μM
14	Dextromethorphan hydrobromide	10 μM
15	2.3-Pyridinedicarboxylic acid(DPA)	10 μM
16	R-(-)-Deprenyl hydrochloride(Selegiline hydrochloride)	10 μM
17	NS-398	10 μM
18	4-Aminobenzoic acid(PABA,Vitamin Bx, Vitamin H1)	10 μM
19	Biotin	10 μM
20	D-Pantothenic acid hemicalcium salt(Vitamin B5)	10 μM
21	Chondroitin sulfate A sodium salt from bovine tracha(Glycosaminoglycans)	10 μg/mL
22	Ebselen	10 μM
23	PPBP maleate(4-PPBP maleate)	10 μM
24	Minocycline hydrochloride	10 μM
25	Pravastatin sodium salt hydrate	10 μM
26	*N*-tert-Butyl-alpha-phenylnitrine(PBN)	10 μM
27	Curcumin	10 μM
28	TRO19622(Olesoxime)	10 μM
29	Pyridoxamine dihydrochloride	10 μM
30	Pyridoxal hydrochloride	10 μM
31	Fibroblast Growth factor-Basic human	100 ng/mL
32	Bryostatin1	100 nM
33	Brain derived neurotrophic factor human	100 ng/mL
34	SRP4988(PEDF)	100 ng/mL
35	Erythropoietin	0.1 UN/mL
36	Clioquinol	10 μM
37	Kenpaullone	10 μM
38	PARP inhibitor iii,DPQ	10 μM
39	Glial Cell Line-derived Neurotrophic Factor human	100 ng/mL
40	Ciliary Neurotrophic Factor, human	100 ng/mL
41	Nitric Oxide Synthase, Neuronal Inhibitor 1(nNOS inhibitor)	10 μM
42	Riluzole	10 μM
43	Creatine	10 μM
44	Anisomycin from streptomyces griseolus	10 μM
45	NE 100 hydrochloride	10 μM
46	Phenytoin	10 μM
47	CsA	300 nM
48	FK506	300 nM
49	Rapamycin	10 μM
50	Docosahexaenoic acid	10 μM
51	GLP-1	50 nM
52	Diazoxide	300 μM
53	Glibenclamide	100 μM
54	2-APB (2-Aminoethoxydiphenyl borate)	200 nM
55	IL1RA	100 ng/mL
56	Retinol	10 μM
57	GW5015-16	10 μM
58	GW9508	10 μM
59	Etomoxir	20 μM
60	Verapamil	20 μM
61	Metformin	44 μM
62	AICAR	10 μM
63	pioglitazone	10 μM

Table S3. Cont.

	Drugs	Treatment conc.
64	Troglitazone	10 μM
65	*N*-Acetyl D-Shingosine	10 μM
66	Dihydroceramide C2	10 μM
67	Fumonisin B1	10 μM
68	Ros inhibitor	100 μM
69	SNAP	1 mM
70	Dantrolene	10 μM
71	Bcl XLBH4 human	1 μM
72	Calp. Inhibitor iii	1 μM
73	salburinal	25 μM